Research Article

Madhu Sharma, Bhupendra K. Sharma*, Anup Kumar, Bandar Almohsen, David Laroze, and Kamil Urbanowicz

Computational simulation of heat transfer and nanofluid flow for two-sided lid-driven square cavity under the influence of magnetic field

https://doi.org/10.1515/phys-2025-0153
received September 11, 2024; accepted January 03, 2025

Abstract: The present study investigates the heat transfer for the unsteady, incompressible, two-dimensional mixed convective copper–water nanofluid flow in a lid-driven square cavity in the presence of the magnetic field. The lid-driven square cavity's top and bottom walls are assumed to be adiabatic. The nanofluid model is developed in ANSYS-FLUENT using Boussinesq approximation. A pressure-based solver with a Semi-Implicit Method for Pressure-Linked Equations algorithm is used to simulate the governing equations of the model. The results obtained from the developed fluid model are examined for the different influential physical parameters to enhance heat transfer from the cavity to the flowing fluid. Qualitative and quantitative results for nanofluid concentration, magnetic field parameter, and Reynolds number are analyzed. A noteworthy observation is that the velocity of the nanofluid reduces with improvement in the magnetic field strength. The findings of the attempt provide the capability of nanofluids in heat transfer, which aids in creating innovative geometries with improved and regulated heat transfer due to applied magnetic fields. This attempt holds potential applications in solar collectors, electrical devices, and the medical field manageable due to the slower fluid flow (nanofluid).

Keywords: mixed convection, nanofluids, square cavity, heat transfer, magnetic field

*** Corresponding author: Bhupendra K. Sharma,** Department of Mathematics, Birla Institute of Technology and Science, Pilani, Rajasthan, India, e-mail: bksharma@pilani.bits-pilani.ac.in
Madhu Sharma: Department of Applied Sciences and Humanities, Bhartiya Institute of Engineering and Technology, Sikar, Rajasthan, India, e-mail: madhusharma5dec@gmail.com
Anup Kumar: Department of Mathematics, Birla Institute of Technology and Science, Pilani, Rajasthan, India, e-mail: yadavanupbalwan1996@gmail.com
Bandar Almohsen: Department of Mathematics, College of Science, King Saud University, P.O. Box 2455, Riyadh 11451, Saudi Arabia, e-mail: balmohsen@ksu.edu.sa
David Laroze: Instituto de Alta Investigación, Universidad de Tarapacá, Casilla 7D, Arica, Chile, e-mail: dlarozen@academicos.uta.cl
Kamil Urbanowicz: Faculty of Mechanical Engineering and Mechatronics, West Pomeranian University of Technology in Szczecin, Al. Piastów 17, 70-310 Szczecin, Poland, e-mail: kamil.urbanowicz@zut.edu.pl

Nomenclature

α	thermal diffusivity
β	thermal expansion coefficient
C	concentration of fluid
Gr	Grashof number
K	thermal conductivity
μ	kinematic viscosity
ϕ	volume fraction
p_{m}	Prandtl number
Re	Reynolds number
ρ	density
$(\rho C_{\mathrm{p}})_{\mathrm{s}}$	heat capacitance of metallic nanoparticle
$(\rho C_{\mathrm{p}})_{\mathrm{f}}$	base fluid heat capacity
$(\rho C_{\mathrm{p}})_{\mathrm{nf}}$	nanofluid heat capacity
t	time
T	temperature of fluid
T_1	temperature of upper wall of tube
U, V	velocity components in the (X, Y) direction
V_{p}	velocity of moving lid
Subscripts and superscripts	
c	cold wall
eff	effective
f	fluid
h	hot wall

nf	nanofluid
s	solid
0	reference value

1 Introduction

Mixed convective heat transfer in a lid-driven cavity finds extensive applications in various fields, ranging from cooling electronic devices to building high-performance insulation, nuclear reactors for multi-shield structures, solar power collectors, float glass production, furnaces, and drying technologies [1–5]. Mixed convective flows in heat transfer, where both forced and natural convection mechanisms coexist, offer several advantages in various engineering applications. Mixed convective flows often result in higher heat transfer rates than pure forced or natural convection. Mixed convective flows are adaptable to different flow configurations, geometries, and boundary conditions. Mixed convective flows promote temperature uniformity in the fluid or around a heated surface and are particularly effective in enclosed spaces or confined geometries. The synergistic effect of forced and natural convection in mixed convective flows improves energy efficiency. Mixed convective flows exhibit adaptability to changing operating conditions, making them a valuable consideration in designing and optimizing heat transfer systems in various engineering applications. Numerous studies have analyzed convective heat transfers within different cavity shapes, such as triangular, trapezoidal, cylindrical, wavy, and square. These investigations are critical for developing a comprehensive understanding of fluid dynamics inside cavities, contributing to thermal enhancement and optimization. Researchers have proposed various strategies to improve specific properties and enhance heat transfer within cavities, which include introducing multiple fins utilizing nanofluids into the cavity [6,7]. A noteworthy study by Kumawat *et al.* [8] on the flow of power-law nanofluid blood two-phase simulations with an intensity of magnetic field through a curved overlapping stenosed artery. Gandhi *et al.* [9] examined the time-variant flow of blood through an artery multi-stenotic mediated by hybrid nanoparticles. In a bifurcated artery with gyrotactic microorganisms, Sharma *et al.* [10] explored entropy formation in a ternary hybrid nanofluid. Additionally, Sharma *et al.* [11] investigated the radiative heat transfer for hybrid nanofluids in solar collectors. Kumar *et al.* [12] focused on the heat transfer analysis for magnetohydrodynamics (MHD) Jeffrey hybrid nanofluid flow in conjunction with a bioconvection mechanism in radiative solar collectors. These studies contribute to the knowledge surrounding mixed convection flow and heat transfer, offering insights into optimization techniques and strategies for enhancing the thermal performance of various applications.

Research on mixed convective flows from the enclosures has attracted significant attention, primarily due to its expanding applications. However, a noticeable gap exists in the investigation of mixed convective heat transfer from enclosures with nanofluids despite the acknowledged potential of incorporating nanoparticles into a fluid to address various heat transfer challenges. Copper (Cu)–water nanofluids, consisting of Cu nanoparticles dispersed in water, have gained significant attention in heat transfer augmentation due to several advantages. Copper nanoparticles have high thermal conductivity, and when dispersed in water, they effectively increase the overall thermal conductivity of the fluid. The presence of Cu nanoparticles in the fluid promotes better heat transfer between the fluid and the surrounding surfaces. This increased heat transfer coefficient enhances the efficiency of various industrial and electronic applications. The nanoparticles tend to agitate and disrupt the fluid flow, promoting better mixing and convective heat transfer. Cu nanoparticles generally exhibit good thermal stability, maintaining their properties at elevated temperatures, which makes them suitable for applications with high-temperature stability electronic systems. This reduces energy consumption and operational costs in applications, which makes Cu–water nanofluids promising candidates for various heat transfer applications across different industries. Introducing nanoparticles alters the fluid's thermo-physical properties, adding complexity to mixed convection dynamics by involving intricate interactions among inertia, viscous, and buoyancy forces. Chaudhary *et al.* [13] explored the radiation effect in MHD mixed convective flow with Ohmic heating, considering both thermal and mass diffusion effects. Muthtamilselvan *et al.* [14] discussed using Cu-water nanofluids to increase heat transmission in a lid-driven enclosure. Valipour and Ghadi [15] specifically examined the nanofluid flow, focusing on the impact of nanoparticle volume fraction on flow patterns. Their findings highlighted observable changes in minimum velocity and recirculation length with an escalation in nanofluid concentration. Sharma *et al.* [16] investigated the minimization of entropy formation in MHD mixed convective flow with endothermic/exothermic catalytic reaction. Additionally, Sharma *et al.* [17] studied the combined effects of thermophoretic diffusion and Brownian motion across an inclined stretched surface with a chemical reaction in mixed convective flow. These studies contribute to understanding mixed convection in nanofluid-filled enclosures, considering various factors such as radiation, nanofluid heat transfer enhancement, and chemical reactions.

Investigations into heat transfer under unsteady regimes with different geometries offer several advantages in understanding and optimizing thermal systems. Unsteady heat transfer is prevalent in many real-world applications, such as transient heating or cooling processes, startup and shutdown of equipment, and rapid changes in environmental conditions. Unsteady regimes often involve transient phenomena, where temperatures, velocities, and thermal gradients change rapidly. Incorporating unsteady heat transfer into predictive models allows for more accurate simulations and predictions of system behavior. Heat transfer studies contribute to the intensification of industrial processes. By optimizing heat transfer under dynamic conditions, it becomes possible to enhance the efficiency of processes like chemical reactions, material processing, and crystallization, leading to improved productivity and resource utilization. Sarkar *et al.* [18] examined the water-Cu nanofluid's mixed convective heat transmission through the cylinder. Their observations revealed the enhancement in Strouhal number with the rise in nanofluid concentration, reducing vortex shedding. In a study by Gorla and Hossain [19], mixed convection flows with nanofluids past a vertical cylinder were explored, highlighting enhanced heat and mass transmission with increased buoyancy ratio parameters. Valipour *et al.* [20] simulated Al_2O_3-water nanofluid in a forced convective fluid flow with heat transmission about a square-shaped cylinder. Increments in drag coefficient, Nusselt number, recirculation length, and pressure coefficient are noted with rising nanofluid concentration. Pourmahmoud *et al.* [21] explored mixed convection heat transmission using nanofluid in a lid-driven cavity, while Bovand *et al.* [22] analyzed the impact of an Al_2O_3-water nanofluid on heat transfer and fluid flow across the equilateral triangled obstacle with varying orientations. In another study by Sharma *et al.* [23], unsteady MHD mixed convection fluid flow with non-uniform heat source/sink and Joule heating was examined. These investigations contribute to understanding mixed convection fluid flows with nanofluids, addressing factors such as unsteady regimes with different geometries.

Magnetic fields influence heat transfer in certain materials through MHD. MHD studies the influences of magnetic fields on electrical conductive fluids. The magnetic field generates Lorentz force in the electrical conductive fluids, which changes the flow patterns due to the magnetic field induced by electric currents. MHD convection alters the temperature distribution within the fluid, impacting heat transfer processes. In this process, a magnetic field changes a material's magnetic entropy, causing it to absorb or release heat. As the magnetic field is varied, the material undergoes a cyclic process of magnetization and demagnetization, leading to changes in temperature. The study of a magnetic field in fluid dynamics for augmenting system performance has become a burgeoning area of research. Several studies have discussed thermal boundary conditions in conjunction with a magnetic field on natural/mixed convection [24–29]. Rashidia *et al.* [30] specifically investigated the unsteady Al_2O_3-water MHD nanofluid flow about a triangled obstacle. Their findings revealed that the higher strength of the magnetic field minimizes the recirculation wake and stabilizes the nanofluid flow. Zhao *et al.* [31] conducted a computational study on on-chip viscoelasticity sensor for biological fluids. Sharma *et al.* [32] introduced the heat transfer characteristics of nanofluids passing over the wall of a heated square cylinder, explicitly altering the front stagnation point by introducing nanofluids. In a numerical study, Sharma *et al.* [33] analyzed entropy generation for blood flow through a curve-shaped artery with the hall effect for power-law MHD fluid. Kumar *et al.* [34] discussed the electromagnetohydrodynamic (EMHD) Jeffrey nanofluid flow in Cu-polyvinyl alcohol/water fluid with an exponential heat source. Khanduri *et al.* [35] conducted a sensitivity analysis using response surface optimization of electroosmotic MHD fluid flow through a curve-shaped stenotic artery. Furthermore, Sharma *et al.* [36] investigated the radiative heat transfer for EMHD Jeffrey nanofluid flow with Joule heating.

In recent years, nanofluids have gained significant attention in heat transfer studies due to their enhanced thermal conductivity compared to conventional fluids. Cu nanoparticles have the potential for improving heat transfer, especially in configurations involving mixed convection, where both forced and natural convection phenomena are present. External magnetic fields influence the nanofluid flow control, as magnetic fields dampen fluid motion by affecting heat transfer. Previous studies have examined nanofluid behavior in various configurations, such as channels and cavities, but often without sufficient focus on the combined effects of magnetic fields and lid-driven cavities. This study addresses these gaps by investigating heat transfer behavior in an unsteady, incompressible, two-dimensional Cu-water nanofluid flowing through a lid-driven square cavity under the influence of a magnetic field. A computational model was developed to simulate this complex flow system using the Boussinesq approximation in ANSYS-FLUENT. A pressure-based solver with the Semi-Implicit Method for Pressure-Linked Equations (SIMPLE) algorithm was applied to simulate the governing equations. Flow parameters like nanofluid concentration, magnetic field strength, and Reynolds number are analyzed, affecting the cavity's heat transfer and flow velocity.

1.1 Novelty and originality

The unique contribution of this study lies in its examination of how magnetic fields modulate heat transfer in nanofluid systems, specifically for the lid-driven square cavity geometry. This focus on magnetic field applications provides insight into the potential use of nanofluids for controlled heat transfer in practical settings like solar collectors, electronic cooling systems, and medical applications. The research demonstrates the application of magnetic fields that regulate the nanofluid flow, leading to applications that require precise thermal management, thus providing a basis for innovative heat transfer solutions in technology and medicine.

Understanding the intricacies of heat transfer in nanofluids is crucial for optimizing thermal performance in various applications. One such application that stands out is the biomedical field, where the manipulation of blood flow during surgeries is a critical factor. The observed reduction in nanofluid velocity under a magnetic field could revolutionize surgical procedures, offering a controlled and manageable environment for medical interventions. The primary objective of this attempt is to advance the current understanding of fluid flow associated with heat transfer phenomena about a bluff body, employing nanofluid. The research involves a numerical exploration of mixed convective heat transmission for Cu-water nanofluid within a lid-driven square-shaped cavity subjected to the influence of an external magnetic field. The investigation explicitly emphasizes nanoparticle concentration's impact on the fluid dynamic characteristics and the heat transmission aspects within the square cavity. By elucidating the interplay of these factors, the objective is to identify conditions that maximize heat transfer from the cavity to the surrounding nanofluid under varying mass fractions and magnetic field parameters.

2 Physical assumptions

Consider a square cavity featuring two-sided lids driven by motion consisting of nanofluid, as depicted in Figure 1. The nanofluid consists of a water-based fluid with Cu nanoparticles. The nanofluid is a homogeneous mixture made from the dispersion of Cu nanoparticles in water. The physical properties of Cu nanoparticles and the water base fluid are assumed to be constant. All physical properties of the nanofluid for the respective concentrations are outlined in Table 1. The cavity is bounded by four walls, with the top and bottom walls taken to be insulated, non-conductive, and resistant to mass transmission. The side wall temperatures are considered constant, as illustrated in Figure 1. In Scenario I, the left wall (cold) moves upward, while the right (hot) moves downward. In Scenario II, the left wall moves downward, while the right one moves upward. In Scenario III, both walls move upward. It is important to note that the moving walls share the same speed in all three scenarios, and the direction of gravitational force is parallel to the moving walls. The schematic diagram of the whole setup is depicted in Figure 1. The investigation

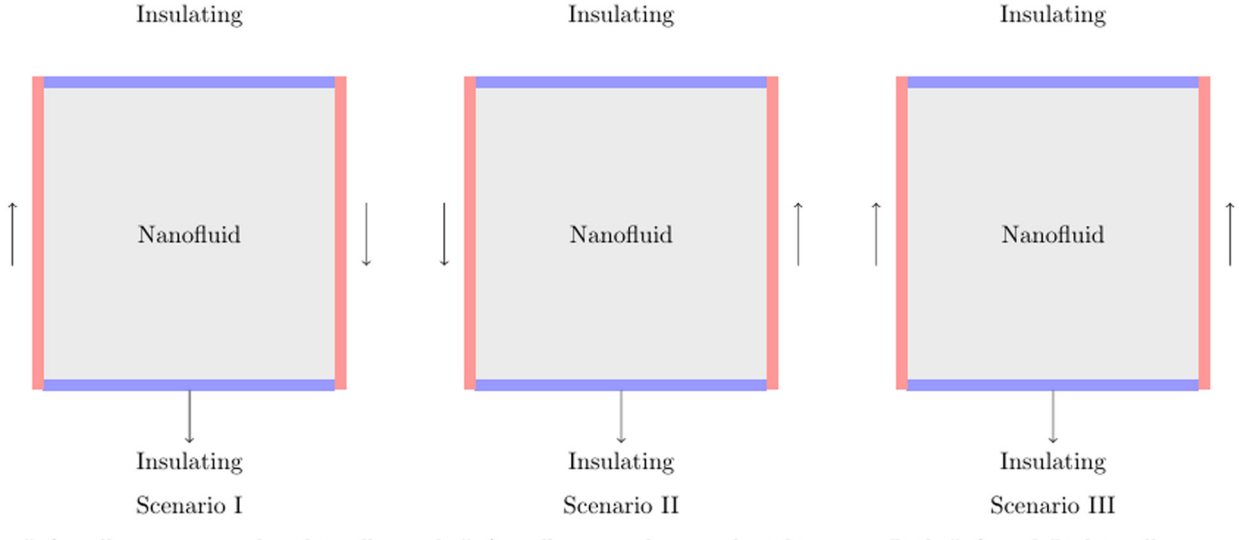

Figure 1: Schematic diagrams for the different cases of the square cavity with two-sided lids and moving side walls filled with nanofluid: (a) left wall moves upward and right wall moves downward, (b) left wall moves downward and right wall moves upward, and (c) both left and right walls move upward.

incorporates the application of continuity, momentum, and energy equations to elucidate the dynamics of an unsteady, two-dimensional flow involving a Newtonian fluid characterized by a constant Fourier property. Moreover, the study posits the negligible influence of radiation heat transfer between surfaces associated with the other heat transfer modes. The following assumptions underlie the analysis:

- The nanofluid inside the enclosure is assumed to be a two-dimensional incompressible Newtonian fluid flow in a laminar pattern.
- Assumptions include uniformity in shape and size for the nanoparticles, nanofluid concentration is taken as constant with various defaults, and the nanofluid mixture is also assumed to be homogeneous.
- Both the fluid and nanoparticle phases are assumed to be in the same phase of thermal equilibrium, flowing with the same momentum and dispersed uniformly in the base fluid.
- The physical properties of the nanofluid remain constant, excluding density variation in the buoyancy force, which is modeled using the Boussinesq approximation.
- Negligible radiation heat transfer is considered from the sides compared to other heat transfer modes.

The Lorentz force easily controls the dynamics of conducting fluids due to a magnetic field, and it has a significant role in heat and mass transfer. The Lorentz force F_L is exerted on a charged particle due to electric and magnetic fields when applied to a continuum (such as MHD in a conducting fluid), introduced in the momentum equations that account for the electromagnetic forces.

2.1 Derivation of Lorentz force term

The Lorentz force F_L for a conducting fluid in the presence of an electric field $\vec{E}$ and a magnetic field $\vec{B}$ is given by:

$$\vec{F}_L = \vec{J} \times \vec{B},$$

where $\vec{J}$ is the current density vector, $\vec{B}$ is the magnetic field vector. Relationship between current density and electric field using Ohm's law for a conductive fluid, the current density $\vec{J}$ can be expressed as

$$\vec{J} = \sigma(\vec{E} + \vec{u} \times \vec{B}),$$

where σ is the electrical conductivity of the fluid, $\vec{u}$ is the fluid's velocity field. Substituting $\vec{J}$ in the Lorentz force expression, the Lorentz force per unit volume can be written as

$$\vec{F}_L = \sigma(\vec{E} + \vec{u} \times \vec{B}) \times \vec{B}.$$

However, for fluid flows with high conductive properties, a small magnetic field can produce a significant Lorentz force that can control the flow dynamics easily; therefore, there is no need for an electric field. In this case, the Lorentz force produced due to the applied magnetic field is

$$\vec{F}_L = \sigma(\vec{u} \times \vec{B}) \times \vec{B}.$$

Based on the above considerations, the governing equations for continuity, momentum, and thermal energy in the laminar pattern are expressed as

$$\frac{\partial U}{\partial X} + \frac{\partial V}{\partial Y} = 0, \tag{1}$$

$$\begin{aligned}\frac{\partial U}{\partial t} + \frac{\partial UU}{\partial X} + \frac{\partial UV}{\partial Y} &= \frac{-1}{\rho_{nf,0}}\frac{\partial P}{\partial X} + \frac{\mu_{eff}}{\rho_{nf,0}} \times \left(\frac{\partial^2 U}{\partial X^2} + \frac{\partial^2 U}{\partial Y^2}\right) \\ &\quad + \mu_0 M\frac{\partial \bar{H}}{\partial X} - \sigma_{nf}B_Y^2 U + \sigma_{nf}B_X B_Y V,\end{aligned} \tag{2}$$

$$\begin{aligned}\frac{\partial V}{\partial t} + \frac{\partial UV}{\partial X} + \frac{\partial VV}{\partial Y} &= \frac{-1}{\rho_{nf,0}}\frac{\partial P}{\partial Y} + \frac{\mu_{eff}}{\rho_{nf,0}}\left(\frac{\partial^2 V}{\partial Y^2} + \frac{\partial^2 V}{\partial X^2}\right) \\ &\quad + \frac{1}{\rho_{nf,0}}[\phi\rho_{s,0}\beta_p + (1-\phi)\rho_{f,0}\beta_f]g(T - T_c) \\ &\quad + \mu_0 M\frac{\partial \bar{H}}{\partial Y} - \sigma_{nf}B_X^2 V + \sigma_{nf}B_X B_Y U\end{aligned} \tag{3}$$

$$\frac{\partial T}{\partial t} + \frac{\partial UT}{\partial X} + \frac{\partial TV}{\partial X} = \alpha_{nf}\left(\frac{\partial^2 T}{\partial X^2} + \frac{\partial^2 T}{\partial Y^2}\right), \tag{4}$$

where $\alpha_{nf} = \frac{K_{eff}}{(\rho C_p)_{nf,0}}$, U and V are the horizontal and vertical velocity components, respectively, T is the temperature, g is the gravity, P is the pressure, μ_{eff} is the dynamic

Table 1: Physical properties of nanofluids and their components with respective mass fraction

Properties	Water (base fluid)	Copper	0% (mass fraction)	1% (mass fraction)	2% (mass fraction)
Density	998.2	8,978	998.2	1796.18	2594.16
Specific heat	4,182	381	4,182	2282.11	1023.4
Thermal conductivity	0.6	387.6	0.6	0.8	1.047
Viscosity	0.001003	—	0.001003	0.00131	0.00175

viscosity, ρ_{nf} is the nanofluid density, β is the thermal expansion coefficient, suffixes p and f denote the nanoparticle and heat transfer fluid, respectively, and $(\rho C_p)_{nf}$ is the nanofluid heat capacity. In cases where the various properties of both the metal nanoparticles suspended and base fluid are known, it becomes necessary to compute the physical properties of the nanofluid. The subsequent equations facilitate this calculation. The symbol nf denotes the nanofluid's effective properties, derived based on the nanoparticle concentration in the base fluid. The nanofluid dynamic viscosity is determined using the Brinkmann model [37], while the thermal conductivity is computed using the Maxwell model [38–40]. The expressions employed to evaluate the nanofluid properties are discussed below.

The relationship for effective viscosity in this context, as provided by Brinkman [37], is utilized and expressed as follows:

$$\mu_{nf} = \frac{\mu_f}{(1-\phi)^{2.5}}.$$

The mathematical expression for the nanofluid density is

$$\rho_{nf} = (1-\phi)\rho_f + \phi\rho_p.$$

And the specific heat capacity is evaluated by the relation

$$(\rho C_p)_{nf} = (1-\phi)(\rho C_p)_f + \phi(\rho C_p)_p,$$

as presented by Xuan and Li [7].

The determination of the thermal conductivity of a nanofluid involves the application of Maxwell-Garnett' approximation model (MG model). Specifically designed for a two-component system comprising nanoparticles with a spherical shape, the MG model provides the following expression:

$$\frac{K_{nf}}{K_f} = \frac{(K_p + 2K_f) - 2\phi(K_f - K_p)}{(K_p + 2K_f) + \phi(K_f - K_p)}.$$

For the above assumptions, the boundary conditions of the fluid model are

$$\begin{aligned}
&I. \quad U = 0,\ V = 1\ (\text{or } -1) \text{ for } X = 0,\ 0 \le Y \le 1.\\
&II. \quad U = 0,\ V = 1\ (\text{or } -1) \text{ for } X = 1,\ 0 \le Y \le 1.\\
&III. \quad U = 0,\ V = 1 \text{ for } X = 0,\ 0 \le Y \le 1;\\
&\frac{\partial T}{\partial Y} = 0 \text{ for } Y = 0,\ 0 \le X \le 1.\\
&IV. \quad U = 0,\ V = 0 \text{ for } X = 0,\ 0 \le Y \le 1;\\
&\frac{\partial T}{\partial Y} = 0 \text{ for } Y = 1,\ 0 \le X \le 1.
\end{aligned} \tag{5}$$

2.2 Heat transfer

The heat transfer is calculated by the Nusselt number along the heated wall of the cavity

$$\mathrm{Nu} = \frac{h_{nf}H}{k_f},$$

where h_{nf} is the heat transfer coefficient formulated as

$$h_{nf} = \frac{q}{T_H - T_c}.$$

Here, q is the wall heat flux per unit area given by

$$q = -k_{nf}\frac{(T_H - T_c)}{H}\frac{\partial T}{\partial X}\bigg|_{X=0}.$$

As a result,

$$\mathrm{Nu} = -\frac{k_{nf}}{k_f}\left(\frac{\partial T}{\partial X}\right).$$

3 Numerical procedure

The numerical procedure utilized an advanced computational framework, ANSYS-FLUENT software, which leverages the Finite Volume Method (FVM), a suite of sophisticated techniques for simulating nanofluid flow. ANSYS-FLUENT is a renowned commercial CFD software known for its versatility and robust capabilities in handling complex flow problems to solve the governing equations, typically the Navier-Stokes equations, which follow the conservation of mass, momentum, and energy within a fluid. The steps involving modeling the fluid model and the solution process are presented with the help of a Flowchart as shown in Figure 2.

The spatial discretization aspect of the methodology is achieved by applying the second-order upwind scheme to enhance accuracy by considering the directional characteristics of fluid flow. The coupling of velocity and pressure is fundamental in fluid flow simulations. A pressure-based solver is employed in this numerical procedure, and the coupling is managed using the SIMPLE algorithm. The SIMPLE algorithm is an iterative approach that alternates between solving for velocity and pressure fields, ensuring a consistent and physically meaningful solution. This iterative process is critical for capturing the intricacies of the pressure-velocity coupling, which is essential for accurately representing fluid dynamics. Convergence criteria play a pivotal role in determining the accuracy and reliability of the numerical solution. The specified error

tolerances of 10^{-7} for the continuity and momentum equations and 10^{-8} for the energy equation act as thresholds for the iterative solution process. Convergence is declared when the changes in these variables lie below the stipulated tolerance values. This meticulous convergence control is crucial for affirming the stability and accuracy of the obtained solution. This numerical procedure combines the computational power of ANSYS-FLUENT with the precision of the FVM second-order upwind scheme, and the sophistication of the SIMPLE algorithm for pressure-velocity coupling. The stringent convergence criteria ensure that the simulation results meet high accuracy standards and provide a reliable and physically meaningful representation of fluid flow phenomena. This comprehensive approach is essential for tackling complex fluid dynamics problems in various engineering and scientific applications.

3.1 Validation

After implementing the methodology mentioned above, the numerical outcomes obtained for the current investigation are validated with the existing attempt of Alsabery *et al.* [41] from the available literature. The numerical results are validated by neglecting the extra assumptions and parameters of the study of Alsabery *et al.* [41]. The novel assumptions and parameters that differ from the existing

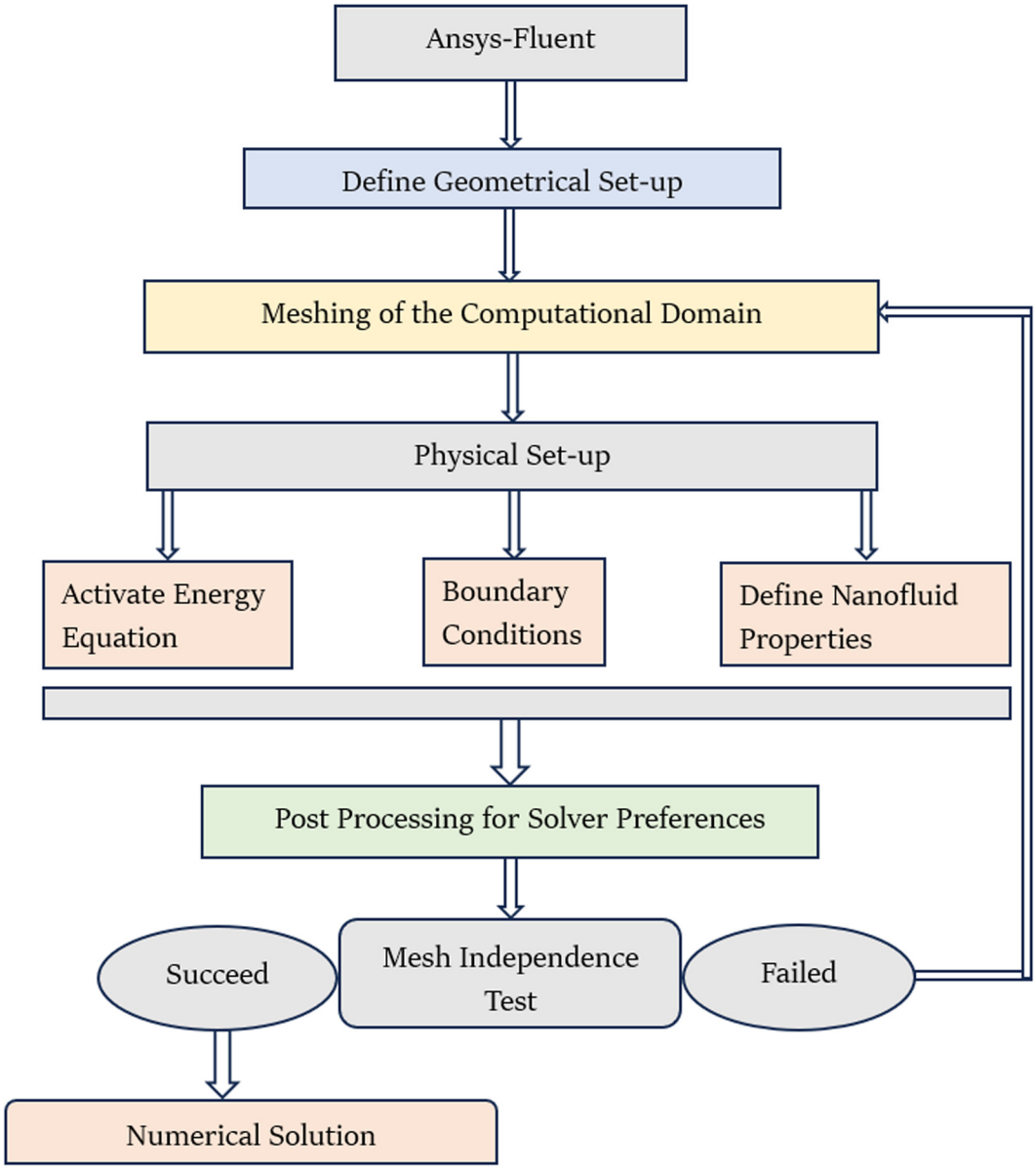

Figure 2: Flow Chart presenting the modeling and solution procedure.

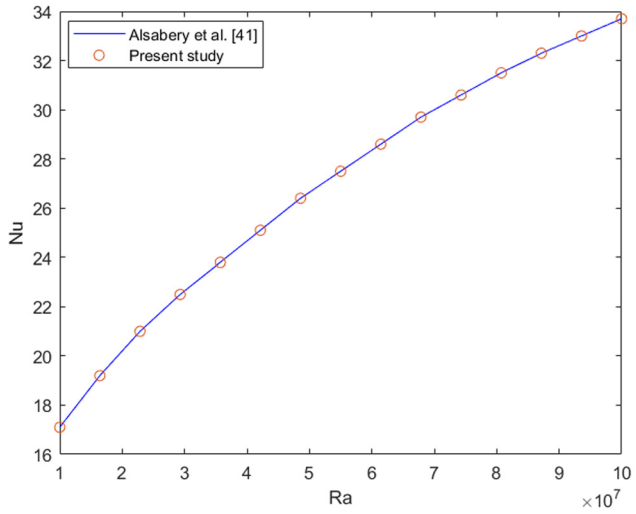

Figure 3: Validation plot for the numerical outcomes of the current investigation with existing literature by Alsabery *et al.* [41].

attempt are considered zero for validation purposes. The numerical outcomes for the Nusselt number are validated and are shown in Figure 3, which reveals that the outcomes agree with the validation. Then, the simulations proceeded further to perform the parametric analysis of the article.

4 Graphical results

The investigation encompasses a range of parameters crucial for understanding heat transfer characteristics in the nanofluid-filled cavity. The nanofluid concentration, magnetic field parameter, and Reynolds number are key variables. The Nusselt number, a fundamental indicator of heat transfer by convection, is analyzed concerning these parameters to quantify the system's thermal performance. This section shows the numerical findings related to the mixed convective fluid flow and characteristics of heat transfer for Cu–water nanofluid within a lid-driven square cavity subjected to an applied magnetic field. The analysis pertains to the third scenario, wherein both vertical walls move upward, resulting in the synergy of buoyancy and shear forces along the right wall. In contrast, the left wall experiences the contrary effect. Consequently, it is anticipated that the predominant circulation will occur on the right side of the cavity. The defaults of the considered influential physical parameters are Ri = 0.1, Gr = 10^4, Pr = 0.67, ϕ = 0, 1, 2%. The graphs for the same have been shown below.

The velocity profile for various mass fractions is illustrated in Figure 4. As the intensity of the applied magnetic field increases, the velocity decreases for each mass fraction. Notably, this effect is most pronounced when the mass fraction of Cu is at its highest value. This implies that a stronger magnetic field corresponds to a more significant decrease in velocity. Also, the velocity of the nanofluid decreases with an increase in the nanofluid concentration. This is due to the effect of viscosity influenced by the concentration of the nanoparticles. A higher concentration of the nanoparticles enhances the viscosity of the nanofluid, and highly viscous fluid exhibits lesser momentum in the fluid flow.

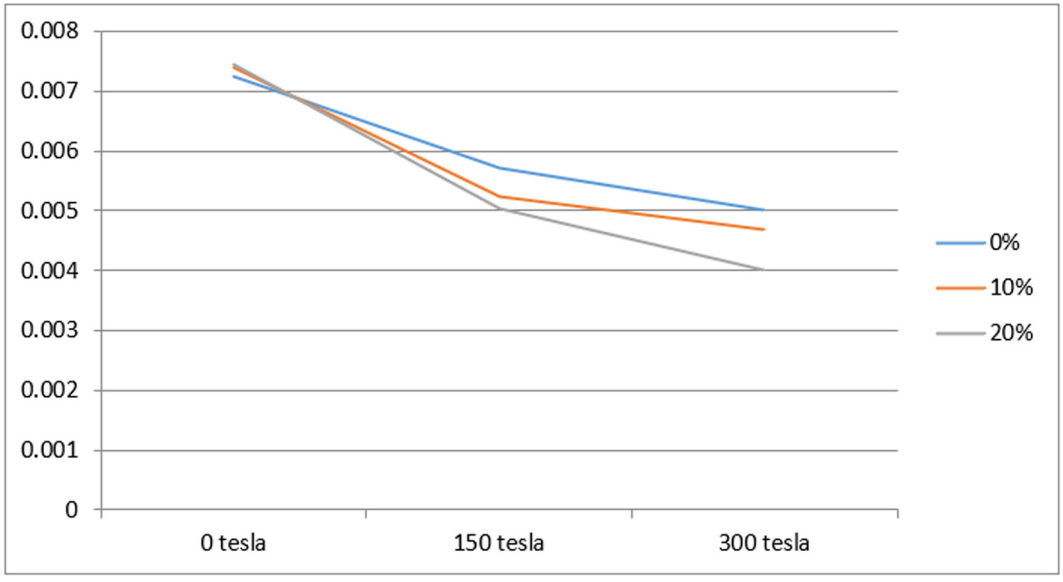

Figure 4: Velocity profile for different values of mass fractions.

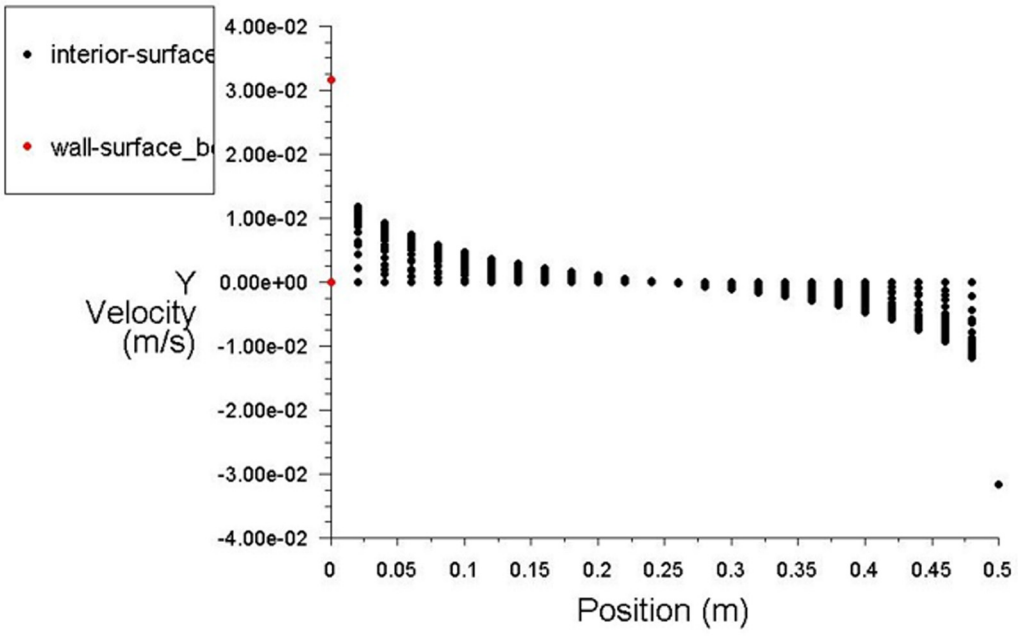

Figure 5: *Y*-velocity trend for different mass fractions.

Additionally, Figure 5 displays the velocity trend for all cases studied. The observed outcome can be readily understood, as the left wall's upward and the right wall's downward motion result in a gradual shift of fluid velocity in the *y*-direction from positive to negative as we traverse from x = 0 m to x = 0.5 m. Moving on to a pivotal aspect of the current investigation, we delve into the variation in heat transfer rate concerning mass fraction and magnetic field. The depicted trend illustrates the change in the Nusselt number within the square cavity, a direct indicator of the heat transfer rate. A more significant Nusselt number corresponds to a greater heat transfer coefficient, indicative of increased heat transfer. The behavior of the Nusselt number for different input parameters is presented in Figure 6. The

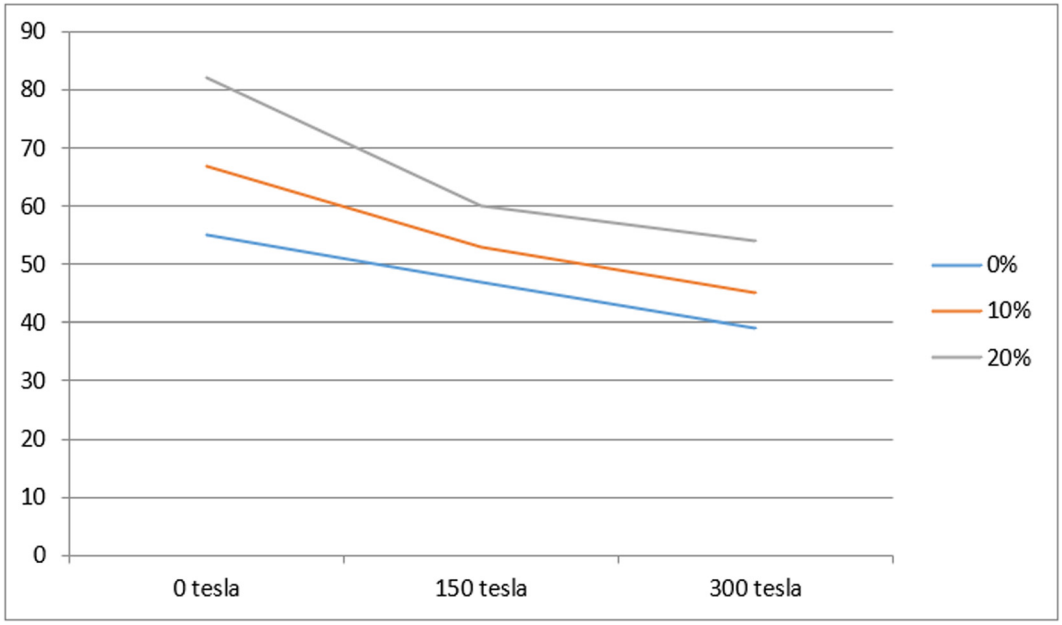

Figure 6: Nusselt number variation with mass fraction and magnetic field.

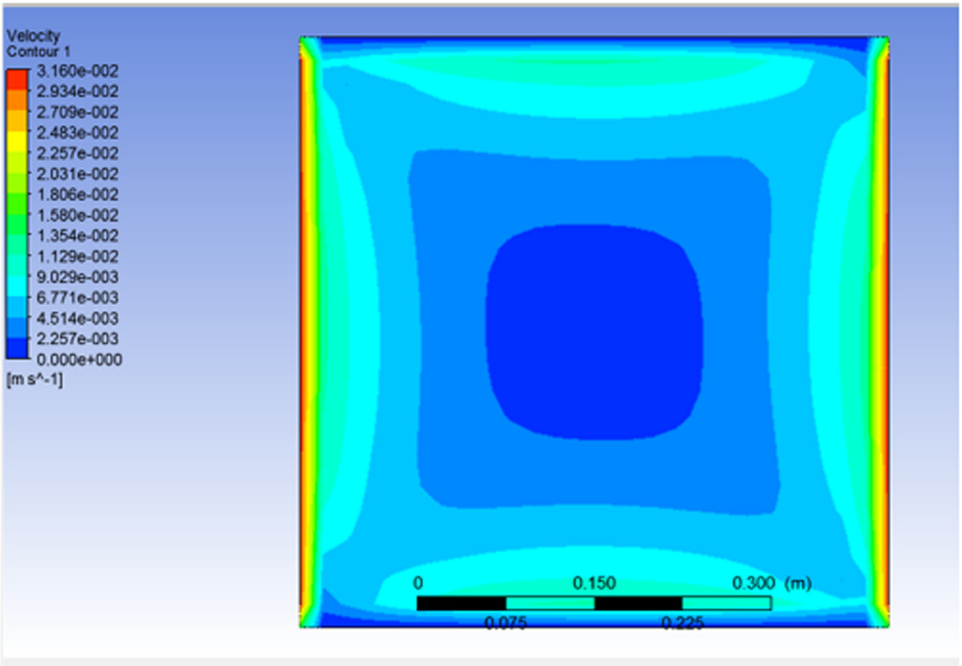

Figure 7: Velocity contour for mass fraction 0% and magnetic field 0 T.

Figure reveals that the magnetic field to the enclosure supresses the velocity profile due to the Lorentz force, which results in a notable decrease in convection intensity. Consequently, the Nusselt number shows a declining trend with the magnetic field parameter enhancement. The escalation in the thermal boundary layer due to mass fraction is attributed to the higher thermal conductivity of the nanofluid. Increased thermal conductivity corresponds to higher thermal diffusivity, leading to reduced temperature gradients and an enlargement of the boundary thickness.

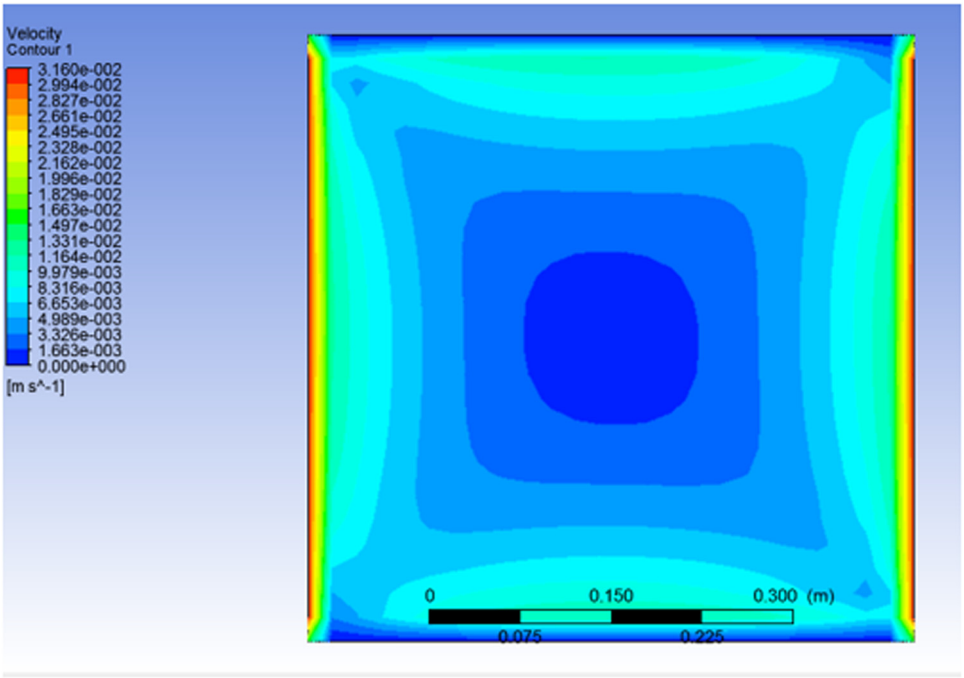

Figure 8: Velocity contour for mass fraction 0% and magnetic field 150 T.

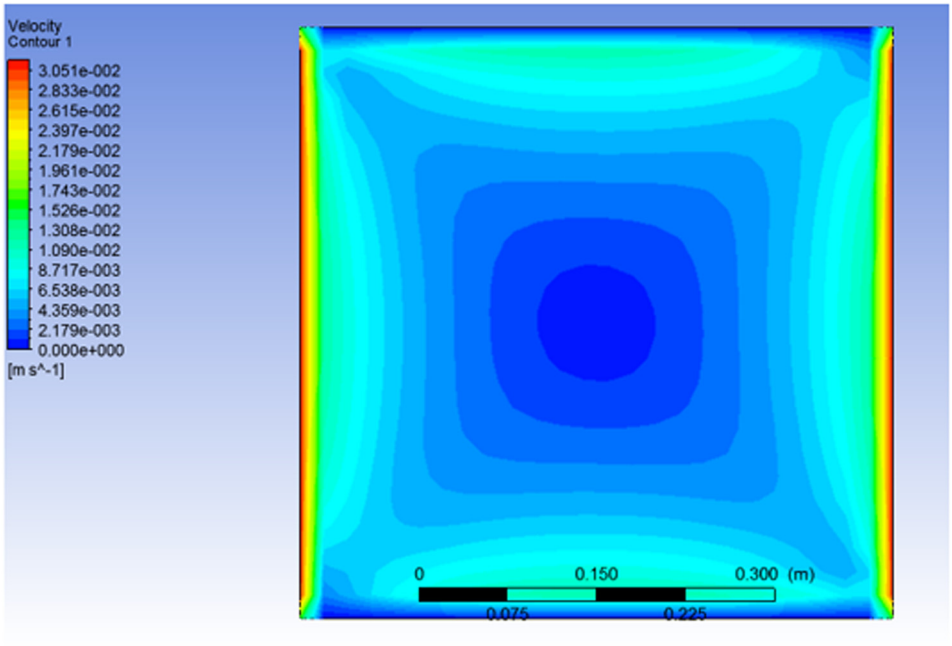

Figure 9: Velocity contour for mass fraction 0% and magnetic field 300 T.

Although the escalating thermal boundary layer thickness drops the Nusselt number, it is important to note that the Nusselt number is the product of the temperature gradient and the heat transfer coefficient. It is observed that the lesser thermal gradients due to the presence of nanoparticles are significantly smaller than the thermal conductivity ratio-consequently, an increase in mass fraction results in a reduction in the Nusselt number.

Figures 7–9 depict velocity contours corresponding to various levels of magnetic field strength. The magnetic field intensity values considered are 0, 150, and 300 T, accompanied by 0% mass fraction. Notably, a discernible

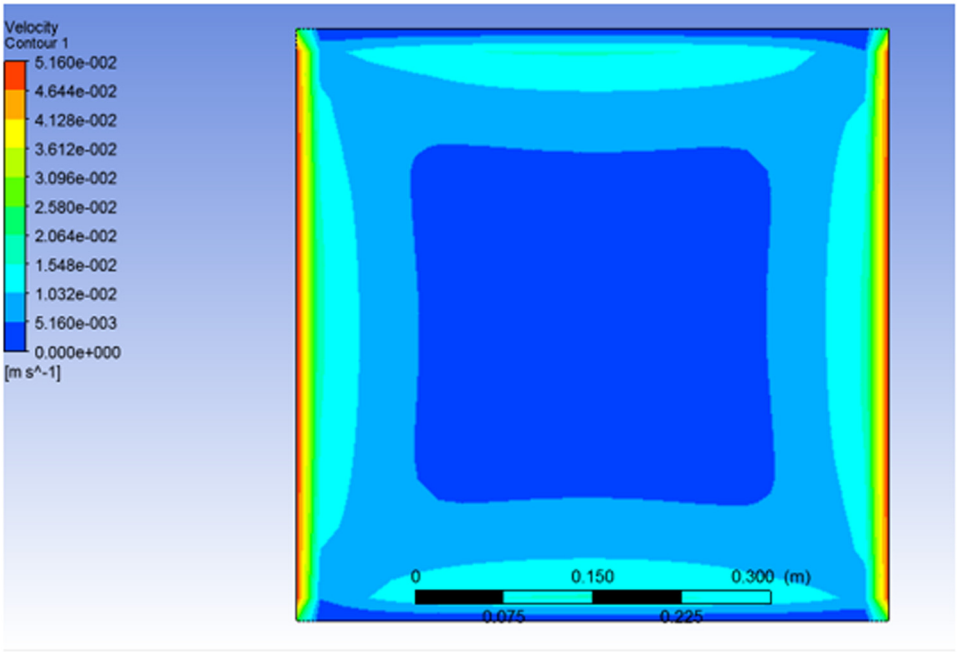

Figure 10: Velocity contour for mass fraction 10% and magnetic field 0 T.

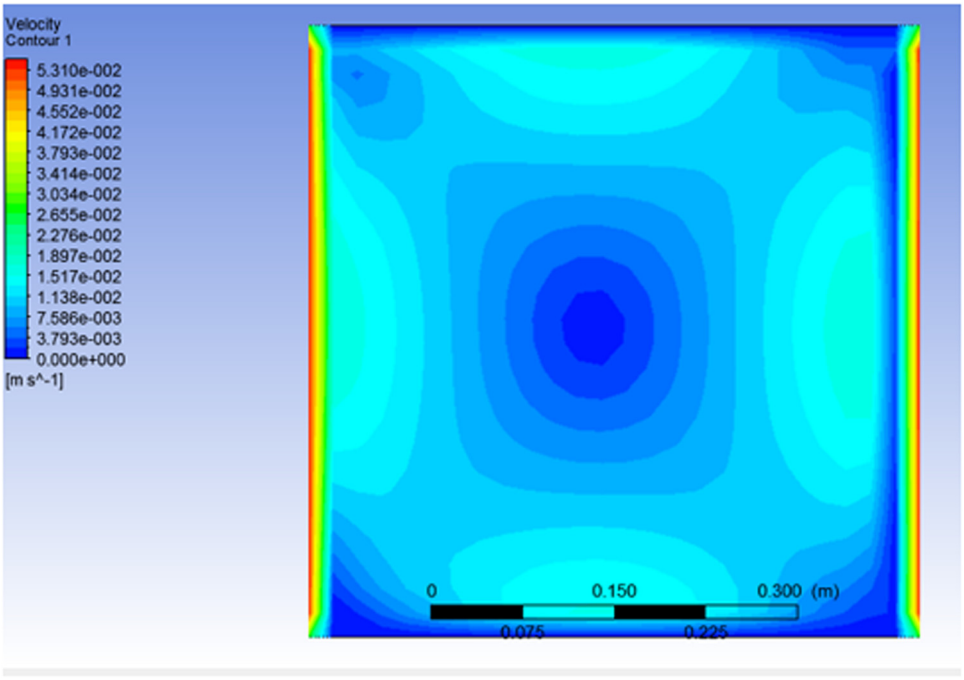

Figure 11: Velocity contour for mass fraction 10% and magnetic field 150 T.

reduction in fluid velocity is observed with the augmentation of the magnetic field. This observation aligns with existing literature, validating the consistency of the simulation outcomes with prior research. The phenomenon can be elucidated as follows: as water possesses diamagnetic properties, it inherently resists the influence of the applied magnetic field, resulting in a gradual decrease in velocity as the magnetic field strength escalates.

The findings about a 1% mass fraction of Cu nanofluid are elucidated in Figures 10–12, incorporating velocity contours. The flow velocity at each instance is explicitly delineated, with specific reference to the movement of the left

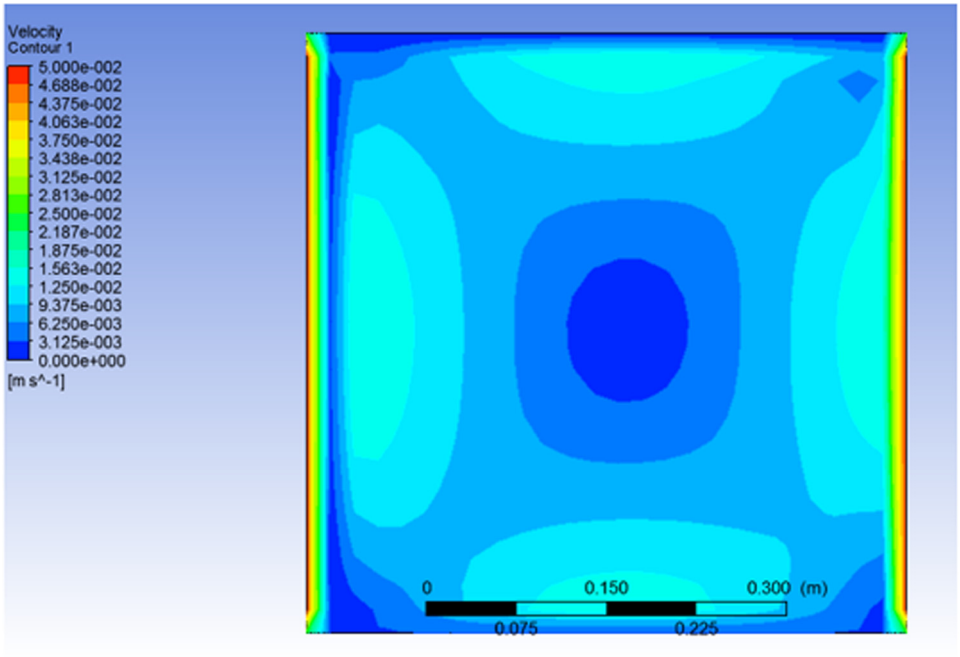

Figure 12: Velocity contour for mass fraction 10% and magnetic field 300 T.

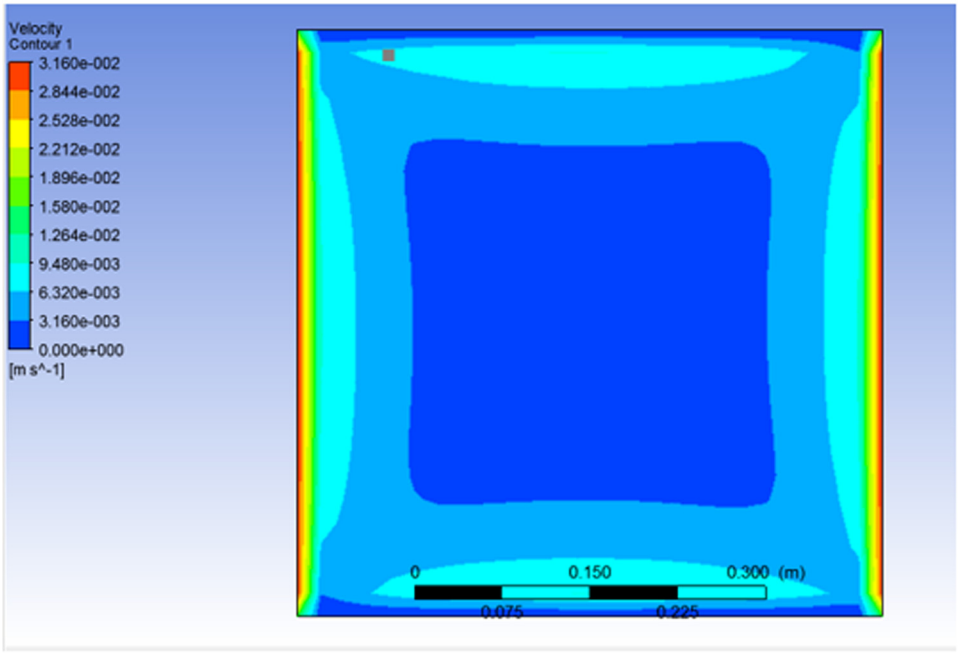

Figure 13: Velocity contour for mass fraction 2% and magnetic field 0 T.

vertical wall (hot, 343 K) in the positive y direction at a rate of 0.00316 m/s, and the right vertical wall (cold, 300 K) in the negative y direction, also at a speed of 0.00316 m/s. The velocity contour analysis reveals a predominant clockwise recirculating eddy encompassing a significant portion of the cavity. Concurrently, a secondary eddy manifests in a counter-clockwise direction at the right corner of the bottom. With an escalation in magnetic field intensity, the secondary eddy gradually enlarges while the primary eddy diminishes in size. Isotherm representations indicate that the magnetic field exerts a suppressive influence on the convective heat transfer mechanism. This is attributed to the emergence of uniformly distributed isotherms within the cavity, particularly at the bottom.

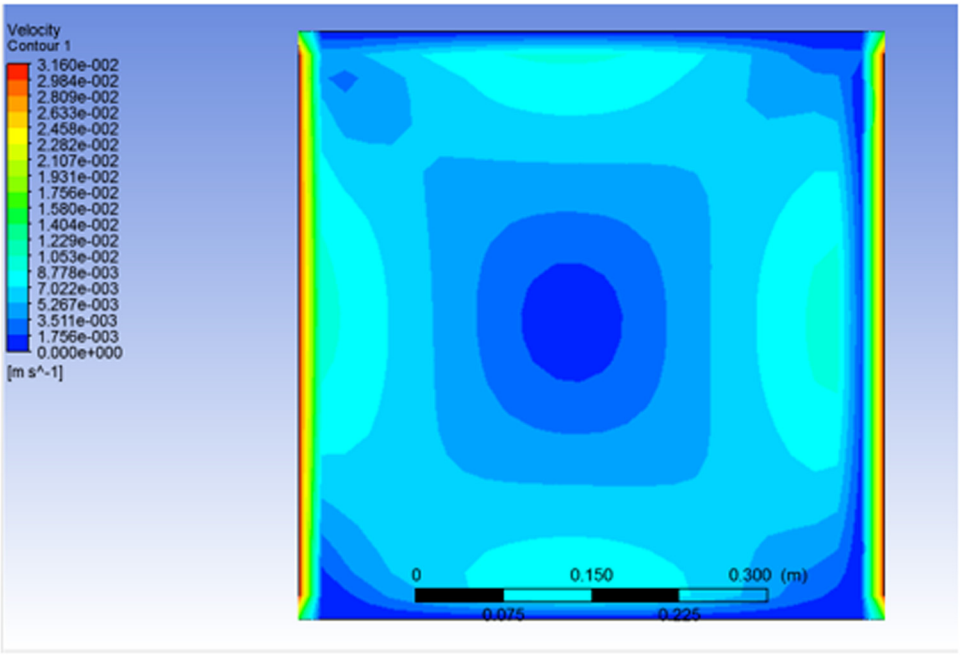

Figure 14: Velocity contour for mass fraction 2% and magnetic field 150 T.

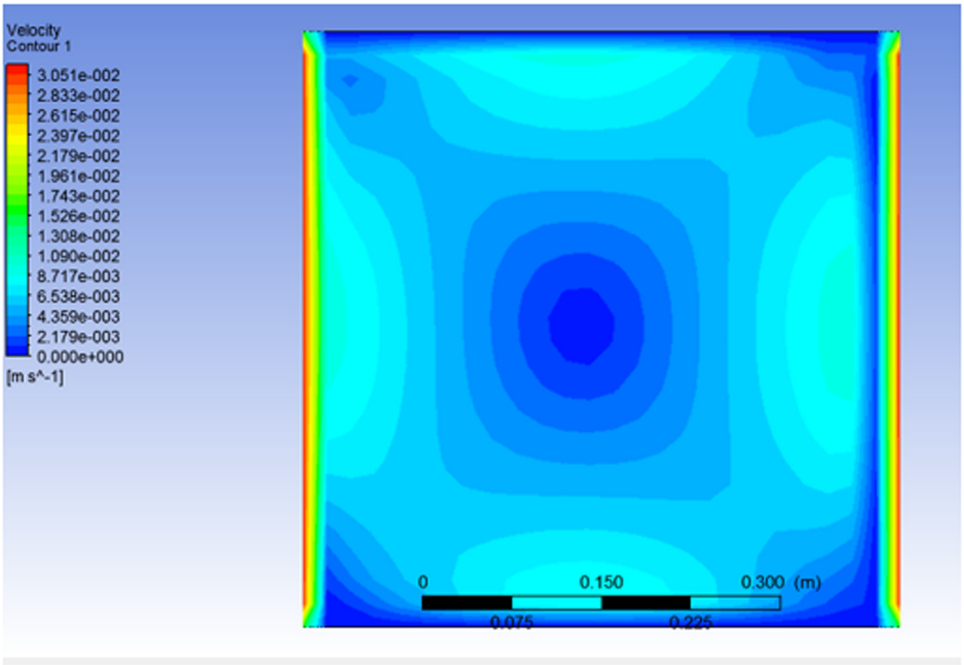

Figure 15: Velocity contour for mass fraction 2% and magnetic field 300 T.

The velocity contours for a nanofluid with a mass concentration of 2% under varying magnetic field strengths are illustrated in Figures 13, 14, 15. The contours depict a prevalence of shear effects attributed to the motion of the upper lid without a magnetic field. A predominant clockwise recirculating eddy characterizes the fluid flow at 0 T, indicating that the flow is primarily propelled downward by the movement of the top lid. With the introduction of a magnetic field (150 T), the primary recirculating eddy shifts its position, moving closer to the moving wall while gaining strength. Upon further increase in the magnetic field to 300 T, a counter-clockwise recirculating eddy emerges along the bottom wall. The observed reduction in nanofluid velocity for varying magnetic fields opens up avenues for innovative applications in the medical field. Controlled blood flow during surgeries is critical for ensuring precision and minimizing risks. The findings of this study, if validated experimentally, could contribute to the development of advanced medical devices and procedures, making surgeries more manageable and enhancing patient outcomes.

5 Conclusion

The current attempt investigates the heat transmission for the unsteady, incompressible, two-dimensional mixed convective Cu–water nanofluid flow with the influence of a magnetic field over a lid-driven square cavity. By comprehensively examining the impact of mass fraction, magnetic fields, and Reynolds number, the study provides a holistic understanding of the factors shaping convective heat transfer in Cu–water nanofluids. These insights are pivotal for developing novel geometries to harness enhanced and controlled heat transfer, with applications in diverse fields such as solar collectors and electronic devices. The model is developed using ANSYS-FLUENT for a lid-driven square cavity, and the key findings are summarized as follows:

- The enhancement of Rayleigh number escalates the Nusselt number, *i.e.,* heat transfer rates.
- An escalation in the magnetic field's intensity reduces the velocity profiles for constant mass fractions.
- The fluid velocity reduces with augmenting the mass fraction of the nanofluid.
- Fluid temperature increases with an escalation in the nanofluid concentration.
- The magnetic field absence dominates the shear effect in contour plots.
- Nusselt number diminishes with an improvement in magnetic field strength for all mass fraction ratios.
- Nusselt number drops with an increase in nanoparticle concentration in the nanofluid.

The results of this investigation provide crucial information about the behavior of nanofluids in heat transfer. These findings can be instrumental in making novel

geometries to achieve controlled and improved heat transfer, particularly for applications in solar collectors and electronic devices. This research endeavors to advance our understanding of mixed convection heat transmission in a lid-driven square cavity with Cu–water nanofluids under the effect of a magnetic field. The findings have potential implications in biomedical applications, offering a novel avenue for the controlled manipulation of nanofluid flow. Furthermore, the study contributes to the broader field of nanofluid research by providing valuable insights that can inform the design of innovative geometries for enhanced and controlled heat transfer in various technological applications.

Funding information: D.L. acknowledges partial financial support from Centre of Excellence with BASAL/ANID financing, AFB220001 and FONDECYT 1231020. The research was supported by Researchers Supporting Project number (RSP2025R158), King Saud University, Riyadh, Saudi Arabia. The author B.K.S. expresses his sincere thanks to DST-SERB, New Delhi (Award letter No: MTR/2022/000315) under the MATRICS scheme.

Author contributions: Madhu Sharma: conceptualization, methodology, and writing – original draft. Bhupendra K. Sharma: formal analysis, investigation, and methodology, software. Anup Kumar: methodology, validation, and writing – original draft. Bandar Almohsen: formal analysis, supervision, and funding acquisition. David Laroze: funding acquisition, supervision, writing – review and editing, Kamil Urbanowicz: supervision, funding acquisition, and writing – review and editing. All authors have accepted responsibility for the entire content of this manuscript and approved its submission.

Conflict of interest: The authors state no conflict of interest.

Data availability statement: The data that support the findings of this study are available from the corresponding author upon reasonable request.

References

[1] Poulikakos D, Bejan A. Natural convection experiments in a triangular enclosure. J Heat Transfer. 1983;105:652–5.
[2] Peric M, Natural convection in trapezoidal cavities. Numer Heat Transfer Part A. 1993;24:213–9.
[3] Mao Z, Hosoya N, Maeda S. Flexible electrohydrodynamic fluid-driven valveless water pump via immiscible interface. J Cyborg Bionic Syst. 2024;5:0091.
[4] Borjigin S, Zhao W, Fu W, Liang W, Bai S, Ma J, et al. Review of plate heat exchanger utilized for gases heat exchange. J Renew Sustain Energy Rev. 2025;210:115224.
[5] Mahmud S, Das PK, Hyder N. Laminar natural convection around an isothermal square cylinder at different orientations. Int Commun Heat Mass Transf. 2002;29:993–1003.
[6] Li N, Morozov I, Fu L, Deng W. Unified nonlinear elasto-visco-plastic rheology for bituminous rocks at variable pressure and temperature. J Geophys Res Solid Earth. 2025;130(3):e2024JB029295.
[7] Xuan Y, Li Q. Heat transfer enhancement of nanofluids Int J Heat Fluid Flow. 2000;21:58–64.
[8] Kumawat C, Sharma BK, Muhammad T, Ali L. Computer simulation of two phase power-law nanofluid of blood flow through a curved overlapping stenosed artery with induced magnetic field: entropy generation optimization. Int J Numer Methods Heat Fluid Flow. 2023;34(2):741–72.
[9] Gandhi R, Sharma BK, Al-Mdallal QM, Mittal HVR. Entropy generation and shape effects analysis of hybrid nanoparticles (Cu-Al2O3/blood) mediated blood flow through a time-variant multi-stenotic artery. Int J Thermofluids. 2023;18:100336.
[10] Sharma BK, Khanduri U, Gandhi R, Muhammad T. Entropy generation analysis of a ternary hybrid nanofluid (Au-CuO-GO/blood) containing gyrotactic microorganisms in bifurcated artery. Int J Numer Methods Heat Fluid Flow. 2024;34(2):980–1020.
[11] Sharma BK, Kumar A, Almohsen B, Fernandez-Gamiz U. Computational analysis of radiative heat transfer due to rotating tube in parabolic trough solar collectors with Darcy Forchheimer porous medium. Case Stud Therm Eng. 2023;51:103642.
[12] Kumar A, Sharma BK, Bin-Mohsen B, Fernandez-Gamiz U. Statistical analysis of radiative solar trough collectors for MHD Jeffrey hybrid nanofluid flow with gyrotactic microorganism: entropy generation optimization. Int J Numer Meth Heat Fluid Flow. 2024;34(2):948–79.
[13] Chaudhary R, Sharma BK, Jha AK. Radiation effect with simultaneous thermal and mass diffusion in MHD mixed convection flow from a vertical surface with Ohmic heating. Rom J Phys. 2006;51(7/8):715.
[14] Muthtamilselvan M, Kandaswamy P, Lee J. Heat transfer enhancement of Cu-water nanofluids in a lid-driven enclosure. Commun Nonlinear Sci Numer Simulat. 2010;15(6):1501–10.
[15] Valipour MS, Ghadi AZ. Numerical investigation of fluid flow and heat transfer around a solid circular cylinder utilizing nanofluid. Int Comm Heat Mass Transfer. 2011;38:296–1304.
[16] Sharma BK, Gandhi R, Mishra NK, Al-Mdallal QM Entropy generation minimization of higher-order endothermic/exothermic chemical reaction with activation energy on MHD mixed convective flow over a stretching surface. Sci Rep. 2022;12(1):17688.
[17] Sharma BK, Khanduri U, Mishra NK, Mekheimer KS. Combined effect of thermophoresis and Brownian motion on MHD mixed convective flow over an inclined stretching surface with radiation and chemical reaction. Int J Modern Phys B. 2023;37(10):2350095.
[18] Sarkar S, Ganguly S, Biswas G. Mixed convective heat transfer of nanofluids past a circular cylinder in cross flow in unsteady regime. Int J Heat Mass Transfer. 2012;55:4783–99.
[19] Gorla RSR, Hossain A. Mixed convective boundary layer flow over a vertical cylinder embedded in a porous medium saturated with a nanofluid. Int J Numer Methods Heat Fluid Flow. 2013;23(9):1393–405.

[20] Valipour MS, Masoodi R, Rashidi S, Bovand M, Mirhosseini M. A numerical study on convection around a square cylinder using Al_2O_3-H_2O nanofluid. Therm Sci. 2014;18(4):1305–14.
[21] Pourmahmoud N, Ghafouri A, Mirzaee I. Numerical study of mixed convection heat transfer in lid-driven cavity utilizing nanofluid effect of type and model of nanofluid. Therm Sci. 2015;19(5):1575–90.
[22] Bovand M, Rashidi S, Esfahani JA. Enhancement of heat transfer by nanofluids and orientations of the equilateral triangular obstacle. Energy Convers Manag. 2016;97:212–23.
[23] Sharma BK, Gandhi R. Combined effects of Joule heating and non-uniform heat source/sink on unsteady MHD mixed convective flow over a vertical stretching surface embedded in a Darcy Forchheimer porous medium. Propuls Power Res. 2022;11(2):276–92.
[24] Chaudhary RC, Sharma BK. Combined heat and mass transfer by laminar mixed convection flow from a vertical surface with induced magnetic field. J Appl Phys. 2006;99:034901. doi: 10.1063/1.2161817.
[25] Sharma BK, Jha AK, Chaudhary RC. MHD forced flow of a conducting viscous fluid through a porous medium induced by an impervious rotating disk. Rom J Phys. 2007;52(1/2):73–84.
[26] Pirmohammadi M, Ghassemi M, Sheikhzadeh GA. Effect of a magnetic field on buoyancy-driven convection in differentially heated square cavity. IEEE Trans Magn. 2009;45(1):407–11.
[27] Sharma BK, Sharma PK, Chand T, Chaudhary RC. Analytical investigation of the hydromagnetic flow in a porous medium due to periodically heated oscillating plate. Int J Appl Mech Eng. 2012;17(4):1367–75.
[28] Aghaei A, Khorasanizadeh H, Sheikhzadeh G, Abbaszadeh M. Numerical study of magnetic field on mixed convection and entropy generation of nanofluid in a trapezoidal enclosure. J Magn Magn Mater. 2016;403:133–45.
[29] Mishra A, Sharma BK. MHD mixed convection flow in a rotating channel in the presence of an inclined magnetic field with the Hall effect. Thermo Phys. 2017;90(6):1563–74.
[30] Rashidia S, Bovandb M, Esfahania JA. Opposition of MHD and AL_2O_3-water nanofluid flow around a vertex facing triangular obstacle. J Mol Liq. 2016;215:276–84.
[31] Zhao Q, Yan S, Zhang B, Fan K, Zhang J, Li W. An on-chip viscoelasticity sensor for biological fluids. J Cyborg Bionic Syst. 2023;4:0006.
[32] Sharma S, Maiti DK, Alam MM, Sharma BK. Nanofluid flow over a heated square cylinder near a wall under the incident of Couette flow. J Mech Sci Tech. 2018;32(2):659–70.
[33] Sharma BK, Kumawat C, Khanduri U, Mekheimer KS. Numerical investigation of the entropy generation analysis for radiative MHD power-law fluid flow of blood through a curved artery with hall effect. Waves Random Complex Media. 2023;1–38.
[34] Kumar A, Sharma BK, Gandhi R, Mishra NK, Bhatti MM. Response surface optimization for the electromagnetohydrodynamic Cu-polyvinyl alcohol/water Jeffrey nanofluid flow with an exponential heat source. J Magn Magn Mater. 2023;576:170751.
[35] Khanduri U, Sharma BK, Sharma M, Mishra NK, Saleem N. Sensitivity analysis of electroosmotic magnetohydrodynamics fluid flow through the curved stenosis artery with thrombosis by response surface optimization. Alexandr Eng J. 2023;75:1–27.
[36] Sharma BK, Kumar A, Mishra NK, Albaijan I, Fernandez-Gamiz U. Computational analysis of melting radiative heat transfer for solar riga trough collectors of Jeffrey hybrid-nanofluid flow: A new stochastic approach. Case Studies Thermal Eng. 2023;52:103658.
[37] Brinkman HC. The viscosity of concentrated suspensions and solutions. J Chem Phys. 1952;20:571–81.
[38] Maxwell-Garnett J. Colours in metal glasses and in metallic films. Philos Trans R Soc London Ser A. 1904;203:385–420.
[39] Hamilton RL, Crosser OK. Thermal conductivity of heterogeneous two-component systems. Ind Eng Chem Fundamen. 1962;1:187–91.
[40] Das PK, Li X, Liu ZS. Effective transport coefficients in PEM fuel cell catalyst and gas diffusion layers: Beyond Bruggeman approximation. Appl Energy 2010;87:2785–96.
[41] Alsabery AI, Tayebi T, Kadhim HT, Ghalambaz H, Hashim I, Chamkha AJ. Impact of two-phase hybrid nanofluid approach on mixed convection inside wavy lid-driven cavity having localized solid block. J Adv Res. 2021;30:63–74. Elsevier.